

RESEARCH ARTICLE

SUGP2 p.(Arg639Gln) variant is involved in the pathogenesis of hemochromatosis via the CIRBP/BMPER signaling pathway

Yanmeng Li^{1,2}  | Anjian Xu²  | Susu Liu³ | Wei Zhang¹ | Donghu Zhou² | Qin OuYang² | Huaduan Zi² | Bei Zhang² | Ning Zhang¹ | Wei Geng⁴ | Yiming Zhou⁵ | Weijia Duan¹ | Xiaoming Wang¹ | Xinyan Zhao¹ | Xiaojuan Ou¹ | Changfa Fan³ | Jidong Jia¹ | Jian Huang² 

¹Liver Research Center, Beijing Friendship Hospital, Capital Medical University, Beijing Key Laboratory of Translational Medicine on Liver Cirrhosis, National Clinical Research Center for Digestive Diseases, Beijing, China

²Beijing Institute of Clinical Medicine, Beijing Friendship Hospital, Capital Medical University, Beijing, China

³Division of Animal Model Research, Institute for Laboratory Animal Resources, National Institutes for Food and Drug Control (NIFDC), Beijing, China

⁴Department of Gastroenterology, Beijing United Family Hospital, Beijing, China

⁵Department of Liver Disease, The Seventh Medical Center, Chinese PLA General Hospital, Beijing, China

Correspondence

Jian Huang, Beijing Institute of Clinical Medicine, Beijing Friendship Hospital, Capital Medical University, Beijing 100050, China.
Email: huangj1966@hotmail.com

Jidong Jia, Liver Research Center, Beijing Friendship Hospital, Capital Medical University, Beijing Key Laboratory of Translational Medicine on Liver Cirrhosis, National Clinical Research Center for Digestive Diseases, Beijing 100050, China.
Email: jia_jd@ccmu.edu.cn

Changfa Fan, Division of Animal Model Research, Institute for Laboratory Animal Resources, National Institutes for Food and Drug Control (NIFDC), Beijing 102629, China.
Email: fancf@nifdc.org.cn

Funding information

National Natural Science Foundation of China, Grant/Award Number: 81974072; Beijing Municipal Natural Science Foundation, Grant/Award Numbers: 7132058, 7202034; Digestive Medical Coordinated Development Center of Beijing Municipal Administration of Hospitals, Grant/Award Numbers: XXX0101, XXZ0502

Abstract

Pathogenic variants in *HFE* and non-*HFE* genes have been identified in hemochromatosis in different patient populations, but there are still a certain number of patients with unexplained primary iron overload. We recently identified in Chinese patients a recurrent p.(Arg639Gln) variant in SURP and G-patch domain containing 2 (*SUGP2*), a potential mRNA splicing-related factor. However, the target gene of *SUGP2* and affected iron-regulating pathway remains unknown. We aimed to investigate the pathogenicity and underlying mechanism of this variant in hemochromatosis. RNA-seq analysis revealed that *SUGP2* knockdown caused abnormal alternative splicing of *CIRBP* pre-mRNA, resulting in an increased normal splicing form of *CIRBP* V1, which in turn increased the expression of *BMPER* by enhancing its mRNA stability and translation. Furthermore, RNA-protein pull-down and RNA immunoprecipitation assays revealed that *SUGP2* inhibited splicing of *CIRBP* pre-mRNA by a splice site variant at *CIRBP* c.492 and was more susceptible to *CIRBP* c.492 C/C genotype. Cells transfected with *SUGP2* p.(Arg639Gln) vector showed up-regulation of *CIRBP* V1 and *BMPER* expression and down-regulation of pSMAD1/5 and *HAMP* expression. CRISPR-Cas9 mediated *SUGP2* p.(Arg622Gln) knock-in mice showed increased iron accumulation in the liver, higher total serum iron, and decreased serum hepcidin level. A total of 10 of 54 patients with hemochromatosis (18.5%) harbored the *SUGP2* p.

Yanmeng Li, Anjian Xu, and Susu Liu contributed equally to this work.

This is an open access article under the terms of the [Creative Commons Attribution-NonCommercial-NoDerivs](https://creativecommons.org/licenses/by-nc-nd/4.0/) License, which permits use and distribution in any medium, provided the original work is properly cited, the use is non-commercial and no modifications or adaptations are made.

© 2024 The Author(s). *American Journal of Hematology* published by Wiley Periodicals LLC.

(Arg639Gln) variant and carried *CIRBP* c.492 C/C genotype, and had increased *BMPER* expression in the liver. Altogether, the *SUGP2* p.(Arg639Gln) variant down-regulates hepcidin expression through the *SUGP2/CIRBP/BMPER* axis, which may represent a novel pathogenic factor for hemochromatosis.

1 | INTRODUCTION

Hemochromatosis is caused by pathogenic variants in genes regulating iron metabolism and is associated with iron overload characterized by excessive absorption and the toxic accumulation of iron in multiple organs such as liver, pancreas, myocardium, and skin.^{1,2} The liver is the most affected organ where the toxic accumulation of iron may lead to cirrhosis and hepatocellular carcinoma.^{3,4}

Variants in classical hemochromatosis-related genes (*HFE*, *HJV*, *HAMP*, and *TFR2*) in *HFE*-related and non-*HFE*-related hemochromatosis, can cause downregulation of *HAMP/Hepcidin*, a central regulator for iron metabolism through the degradation of ferroportin, whereas variants in *SLC40A1* non-*HFE*-related hemochromatosis can result in a gain of function for ferroportin.⁵⁻⁷ In the Caucasian population, *HFE*-related hemochromatosis is the most frequent type and is caused by a homozygous p.(Cys282Tyr) or compound heterozygous p.(Cys282Tyr)/p.(His63Asp) variants in the *HFE* gene.⁸ However, the morbidity of hemochromatosis is less reported in East Asian countries, where the *HFE* p.(Cys282Tyr) variant is rarely identified. Gene variants in hemochromatosis patients in the Asia-Pacific region are quite different from those in patients from America and European countries, and non-*HFE* variants are the most frequent type of gene variant in hemochromatosis patients.⁹⁻¹¹

Several variants in non-*HFE* genes have been reported in Chinese patients with hemochromatosis, including *HJV* p.(Ile287Ser), p.(Cys321*), and p.(Ile281Thr); *TFR2* p.(Ala356fs*)/p.(Gly430Arg) and p.(Gly430Arg)/p.(Tyr320*); and *SLC40A1* p.(Cys326Phe).¹¹⁻¹⁴ In a multi-center study, we have recently identified a series of variants in hemochromatosis in non-*HFE* genes, including *HJV* p.(His104Arg) and p.(Val274Met); *TFR2* p.(Ala302Glu) and p.(Leu745Arg); and *SLC40A1* p.(Tyr333His).^{15,16} However, there are still many unexplained cases of primary iron overload with no causative variant in known hemochromatosis-related genes. By whole exome sequencing, we have identified novel genetic variants in genes involved in iron metabolism,^{7,15,17} including in *SURP* and G-patch domain containing 2 (*SUGP2*), a known splicing-related factor. The recurrent *SUGP2* p.(Arg639Gln) variant (NM_001017392.5) was observed in patients with primary iron overload in our follow-up study.¹⁵

Removal of intron sequences from nascent transcripts is mediated by the spliceosome, a large multicomponent complex. *SUGP2* encodes a *SURP* and G-patch domain containing 2, which carries an N-terminal region that is rich in arginine/serine residues, indicating *SUGP2* to be a novel pre-mRNA processing factor and a component of the spliceosome.¹⁸ However, few studies have investigated its role as a splicing-related factor. In hereditary myopathy with lactic acidosis, *SUGP2* is reported as one of the five nuclear factors that are associated with

abnormal splicing of intron 4 of iron-sulfur cluster assembly (*ISCU*).¹⁹ However, the role of *SUGP2* in the splicing process remains unknown. Additionally, loss of function of a *SUGP2* paralog, *SUGP1*, stimulates alternative splicing (AS) and decreases the stability of the *HMGCR* transcript, which is involved in the regulation of cholesterol metabolism.²⁰ We have shown that silencing *SUGP2* expression decreases pSMAD1/5 level and *HAMP* expression.¹⁵ However, the role of *SUGP2* in the regulation of iron metabolism, especially the role of the *SUGP2* p.(Arg639Gln) variant in hemochromatosis pathogenesis remain unclear.

In this study, we used in vitro and in vivo models to investigate the role of *SUGP2* in the regulation of iron metabolism and the functional consequence of the *SUGP2* p.(Arg639Gln) variant in hemochromatosis. We found that *SUGP2* splicing targeted the gene of cold-inducible RNA-binding protein (*CIRBP*)²¹⁻²³, thereby regulating the expression of bone morphogenetic protein-binding endothelial regulator (*BMPER*), forming a *SUGP2/CIRBP/BMPER* axis to regulate iron metabolism. Furthermore, the *SUGP2* p.(Arg639Gln) variant may activate splicing by c.492 of *CIRBP* exon 6, resulting in increased expression of the *CIRBP* V1 transcript, thereby upregulating *BMPER* and downregulating *HAMP* expression. This may constitute one of the major etiological factors of hemochromatosis in China.

2 | MATERIALS AND METHODS

2.1 | Clinical samples

Patients with primary iron overload were enrolled at the China Registry of Genetic/Metabolic Liver Diseases (CR-GMLD, Clinicaltrials.gov: NCT03131427) for the genetic analysis of variants in the *SUGP2* gene. Among the enrolled patients, 31 showed variants in hemochromatosis-related genes,¹⁷ and an additional 23 hemochromatosis patients were shown in Table S1. Hemochromatosis was diagnosed based on the American Association for the Study of Liver Diseases 2011 practice guidelines on hemochromatosis.²⁴ Study participants were consented under an institutional review board-approved research protocol.

2.2 | Sanger sequencing for *SUGP2* gene and *CIRBP* c.492T>C variant

Sanger sequencing was conducted as described previously.¹⁷ All exons of *SUGP2* were PCR-amplified with *SUGP2*-associated

boundary regions using primers designed with Primer 6 software (Table S2). In addition, primers were designed also for PCR amplification of the gene sequence between *CIRBP* (NM_001280) exon 6 to 7 (Table S2).

2.3 | Exome sequencing

For the identification of accompanied variation in other iron metabolic related genes in patients with *SUGP2* p.(Arg639Gln) in heterozygosity, exome sequencing was conducted as described previously.¹⁷

2.4 | Cell culture

The human liver cell lines, Huh-7 and HCCLM3, were obtained from the Cell Bank of the Type Culture Collection of the Chinese Academy of Sciences (Shanghai, China). Human HepG2 and Hep3B cell lines were obtained from the Cell Resource Center of the Chinese Academy of Medical Sciences (Beijing, China). Huh-7 and HCCLM3 cells were cultured in Dulbecco's modified Eagle's medium, and HepG2 and Hep3B cells were cultured in minimum essential medium (Sigma, USA) supplemented with 10% fetal bovine serum (Gibco-BRL, USA) and 1% penicillin/streptomycin at 37°C with 5% CO₂. All the above cell lines do not carry the *SUGP2* p.R639Q variant.

2.5 | *SUGP2*, *CIRBP*, and *BMPER* siRNAs treatment and construction and transfection of *CIRBP* and *SUGP2* and *SUGP2* p.(Arg639Gln) plasmids

Huh-7, HCCLM3, Hep3B, and HepG2 cells were transfected with 20 μM siRNAs (*SUGP2* siRNA1 and *SUGP2* siRNA2, Thermo, AM16708) using lipofectamine RNAiMAX Reagent (Invitrogen), and *CIRBP* and *BMPER* were knockdown with *CIRBP*-siRNAs (Sangon Biotech) and *BMPER*-siRNAs (RIBOBIO), respectively. The siRNAs sequences of *SUGP2*, *CIRBP*, and *BMPER* are shown in Table S3. The expression plasmid for full-length human *CIRBP* transcript V1 (NM_001280.3) and V3 (NM_001300829.2), wild-type and mutant [harboring p.(Arg639Gln)] *SUGP2* were constructed from the pcDNA3.1 plasmid using the QuikChange Lightning Site-Directed Mutagenesis Kit (Agilent Technologies). Transient transfection was performed with Roche Transfection Reagent (X-tremeGENE Transfection Reagent, Roche) according to the manufacturer's protocol.

2.6 | RNA sequencing

To analyze the AS event and the differentially expressed genes related to iron regulation caused by *SUGP2* silencing in Huh-7 cells, RNA-seq

was conducted as described previously.²⁵ Genes with AS were screened using rMATs software (<http://rmatseq.sourceforge.net/>).

2.7 | Mini-gene assay

Mini-gene splicing vectors were constructed to confirm the AS caused by *SUGP2* siRNAs and the *SUGP2* p.(Arg639Gln) mutant. The sequence between exon 6 and exon 7 of *CIRBP* was synthesized and cloned into the pET01 vector (MoBiTec GmbH, Gottingen, Germany). Cells were transfected with the pET01-*CIRBP* vector using Lipofectamine LTX Reagent (Thermo Fisher Scientific, CA, USA) and treated with *SUGP2* siRNAs or transfected with the *SUGP2* p.(Arg639Gln) mutant. After 24 h, the cells were harvested and total RNA was isolated using TRIzol RNA Isolation Reagent (Invitrogen, CA, USA) and reverse-transcribed to cDNA using a Prime-Script™ RT Reagent Kit (Takara, Shiga, Japan). After PCR amplification using Premix Taq (Takara), agarose gel electrophoresis was performed to identify the splicing changes. Sanger sequencing was performed by Tianyi Huiyuan Biotech Co., Ltd. (Wuhan, China). The primers used were: pET01-Fw, 5'-ATAGCAGCCGGAGTCAGAGT-3' and pET01-Rv, 5'-TTCAGC-GAAGCTCCCAAT-3'.

2.8 | RNA-protein pull-down and mass spectrometry

RNA-pull-down was performed using a PureBinding™ RNA-Protein Pull-Down Kit (Genesee, cat. no. P0201) according to the manufacturer's instructions. Briefly, nuclear extracts were prepared from Huh-7 cells. Mutant and wild-type RNA oligomers (5'-ACAGAGACA-GUUAU/CGACAGUUACGGUA-3') corresponding to *CIRBP* c.492 T/C were designed, synthesized, and end-labeled. The RNA probes were then incubated with beads and Huh-7 cells nuclear extracts. Protein bound to the RNA probes was purified according to the manufacturer's instructions. Eluted protein-RNA complexes were separated on a precast gel and detected by Western blot for *SUGP2*. Bands were excised and subjected to mass spectrometry (MS) to identify proteins binding to the *CIRBP* splicing site. The MS analysis and protein identification were performed by Medical Experimental and Test Center, Capital Medical University (Beijing, China).

2.9 | RNA immunoprecipitation assays

Huh-7 cells were transfected with *SUGP2* plasmids for 48 h. RIP assays were performed using the Imprint® RNA Immunoprecipitation Kit (Sigma-Aldrich, USA), following the manufacturer's instructions. Acquired RNA was subjected to RT-PCR. PCR products were separated by electrophoresis and sequenced. *CIRBP* primers (*CIRBP*-h F/R-6-7) used for RT-PCR and Sanger sequencing are presented in Table S4.

2.10 | Analysis of mRNA stability of *BMPER*

Huh-7 cells transfected with *CIRBP* V1 and *SUGP2* p.(Arg639Gln) mutant plasmid were grown to 70% confluency before being trypsinized and transferred to 12-well plates at 250 000 cells per well. After 48 h, actinomycin D (1 µg/mL, MedChemExpress) was added to the cells incubated for 0, 1, 3, 6, 12, and 24 h. The cells were harvested for RNA extraction, and *BMPER* (NC_000075.7) mRNA was detected by q-RT-PCR.

2.11 | Generation of *Sugp2*^{-/-} and *Sugp2*^{R622Q} mice

Wild-type (WT) C57BL/6 mice and ICR mice were supplied by the Institute for Laboratory Animal Resources, National Institutes for Food and Drug Control (Beijing, China). All studies were conducted in compliance with the "Guide for the Care and Use of Laboratory Animals." The license number of the Animal Use Certificate is 23-2023.

The *SUGP2* knock-out (*Sugp2*^{-/-}) mouse was constructed using CRISPR/Cas9 technology. Two sgRNAs target exon 2 of *Sugp2* were designed (sgRNA1: AGGCACTCTACTAGGAAAGG and sgRNA2: GGAGTGATTCCTACTAGACAT).

For the generation of *Sugp2*^{R639Q} knock-in mouse, analysis of human (transcript-203, NP_001017392.2) and mouse *SUGP2* (transcript-214, NP_001161762.1) protein data showed that the 639th residue (p.Arg639) in human *SUGP2* was conserved as the 622nd residue (p.Arg622) in mouse *Sugp2*. sgRNAs were designed in intron 4 and 5 of *Sugp2* (Table S5), and the sgRNAs with the highest activity were screened using UCATM CRISPR activity assay kit (Biocytogen, China). Then, the target vector was constructed. After confirmation of the target vector by restriction enzyme digestion and sequencing, it was injected into zygotes together with Cas9 mRNA and sgRNA.

For the identification of *Sugp2*^{-/-} and *Sugp2*^{R622Q} mice, a two-step PCR strategy was used. The primers used are shown in Table S6. WT mice yielded an amplified product of 1503 bp, while the *Sugp2* deficient mice failed to amplify the same product as the wild-type. The products amplified from *Sugp2*^{R622Q} mice were 2886 and 3629 bp using primers L-F/L-R and R-F/R-R, respectively (Table S6). Southern blotting for the identification was conducted following manufacturer's instructions (Roche, Basel, Switzerland).

2.12 | Serum iron and ferritin measurements in mice

Blood collected from *Sugp2*^{WT} and *Sugp2*^{R622Q} mutant mice fed a high-iron (Fe) diet (2% carbonyl iron, 2% Fe) for 3 days and 2 weeks.

Serum iron and ferritin measurements were measured as described previously.¹⁷

2.13 | Tissue iron assay and serum hepcidin measurements in mice

Liver tissue from WT and *Sugp2* p.(Arg622Gln) mutant mice fed 2% Fe for 3 days and 2 weeks was homogenized in extracting solution and centrifuged. Tissue iron assay and serum hepcidin measurements in mice were measured as described previously.¹⁷

2.14 | Western blot analysis

Cells and tissues were lysed in lysis buffer (RIPA lysis buffer 10×, Merck) with protease and phosphatase inhibitors and applied to 10% SDS-PAGE gels and probed with antibodies. Blots were visualized using ECL (Bio-Rad) Plus reagents. Antibodies used are listed in Table S7.

2.15 | RNA extraction and quantitative real-time PCR

Total RNA was extracted from liver or cells using Trizol reagent (Sigma) and reverse-transcribed into complementary DNA (Transcriptor cDNA Synth kit 2, Roche). Quantitative real-time PCR was performed using a SYBR green-based assay on the 7500 fast Real-Time System (Applied Biosystems). The sequences of primers for real-time PCR are listed in Table S4.

2.16 | Agarose gel electrophoresis of *CIRBP* RT-PCR products

All the *CIRBP* RT-PCR products were separated by electrophoresis in 2% agarose stained with Midori Green Advance DNA Stain solution following manufacturer's instructions (Bio-Rad, Feldkirchen, Germany). Their images were captured and processed in the Gel Doc 2000 system using the Quantity One (Bio-Rad) program. Fragments of DNA were separated along with the size marker (100–2000 bp DNA size marker, Solis BioDyne, Estonia) in every separation round.

2.17 | Immunohistochemistry, histology, and Prussian blue staining for iron measurements

Immunohistochemistry (IHC) analysis of *BMPER*/*Bmper*, histology, and Prussian blue staining for iron measurements was conducted as described previously.¹⁷ Primary antibodies used were the following Table S7. Masson's trichrome was used to evaluate collagen deposition.

2.18 | Statistical analysis

GraphPad software version 8.0 was used to conduct all statistical comparisons. Non-parametric statistics were applied for the comparison of results in all experiments unless stated otherwise. The Wilcoxon signed-rank test was applied to paired data, and the Mann-Whitney test was applied to unpaired data. $p < .05$ was considered to be statistically significant.

3 | RESULTS

3.1 | SUGP2 knockdown caused abnormal AS of *CIRBP* pre-mRNA, resulting in an increased normal splicing form of *CIRBP* V1 associated with down-regulation of *HAMP* expression

To screen the target genes of SUGP2, we conducted RNA sequencing (RNA-seq) of Huh-7 cells treated with SUGP2-siRNAs (siRNA1 and siRNA2). In cells treated with either of the SUGP2-siRNAs and thereby down-regulated *HAMP* expression (Figure S1A-C), SUGP2 knockdown did not affect the splicing of any iron regulation-related genes but caused abnormal AS of two retained introns (RIs) in *CIRBP* and *SUGP2* and one mutually exclusive exons (MXEs) in *VGLL3* (Figure 1A). Specifically, the normal splicing form of *CIRBP* transcript variant V1 (NM_001280.3) was increased, whereas *CIRBP* transcript variant V3 (NM_001300829.2) with intron 6-7 retained was decreased (Figure 1B,C). Further study of the factors with AS showed the *CIRBP* V1 down-regulated *HAMP* expression (Figure 1D).

Furthermore, we conducted a mini-gene assay to verify the increased *CIRBP* V1 caused by SUGP2 knockdown in liver cell lines with different endogenous SUGP2 expression (Figure 1E, Figure S2). Increased expression of the *CIRBP* V1 and/or decreased *CIRBP* V3 were observed in Huh-7, Hep3B, and HCCLM3 cells treated with SUGP2-siRNAs but less increased expression of the *CIRBP* V1 was observed in HepG2 cells (Figure 1F, Figure S3), whereas decreased expression of the *CIRBP* V1 and/or increased *CIRBP* V3 were observed in Huh-7 and Hep3B cells overexpressing SUGP2 (Figure 1G).

The results indicated that the SUGP2 acted as a splicing inhibition factor and loss of SUGP2 function may result in activated splicing and increased expression of the *CIRBP* V1.

3.2 | The SUGP2 inhibited splicing of *CIRBP* pre-mRNA by a splice site variant at *CIRBP* c.492 and *CIRBP* c.492 C/C genotype was more susceptible for SUGP2 function

To further characterize abnormal SUGP2-mediated splicing of the *CIRBP* gene, we determined the gene sequence between *CIRBP* exon 6 and 7 in Huh-7, HCCLM3, Hep3B, and HepG2

cells lines. A *CIRBP* c.492 C/T variant in exon 6, which was close to the 5' Donor site, was identified in HepG2 and Hep3B cells, while Huh-7 and HCCLM3 showed the *CIRBP* c.492 C/C genotype (Figure 1H,I). Interestingly, consistent with a prediction by MutationTaster that *CIRBP* c.492 site may be a potential splicing site for *CIRBP* pre-mRNA (Figure 1J), the knockdown of SUGP2 increased the splicing of *CIRBP* transcript V3 to transcript V1 in *CIRBP* c.492 C/C genotype cell lines compared with in *CIRBP* c.492 T/C genotype cell lines (Figure 1K,L). This indicated that *CIRBP* c.492 C/C genotype is more susceptible for SUGP2 function.

To test this hypothesis, RNA oligomers probes corresponding to the *CIRBP* c.492 site (C/T) were used to conduct RNA-protein pull-down experiments combined with MS. In addition to SUGP2, we identified 234 proteins binding to the *CIRBP* c.492 C/C site, including a series of splicing-related factors (Figure 1M and Figure S4 and Table S8). Notably, compared with the *CIRBP*-C group, results of the *CIRBP*-U group showed significantly elevated interaction between the SUGP2 protein and *CIRBP* transcripts (Figure 1N), indicating that the *CIRBP* c.492 C/C genotype was more susceptible to SUGP2 function as a splicing inhibitor factor.

To further address the direct relationship between SUGP2 protein and *CIRBP* transcripts, we measured the *CIRBP* transcripts bound to SUGP2 protein using RNA-binding protein immunoprecipitation assays. The results showed increased *CIRBP* V3 and decreased *CIRBP* V1 in the cells treated with SUGP2, and the identification of the *CIRBP* transcripts common sequence (Figure 1O), confirming further the direct interaction between the SUGP2 protein and the *CIRBP* transcript and abnormal AS between *CIRBP* exon 6 and 7.

3.3 | SUGP2 knockdown increased BMPER expression, and the *CIRBP* V1 increased the mRNA stability and translation of BMPER and inhibited BMP-SMAD signaling

RNA-seq of SUGP2 knockdown Huh-7 cells showed altered expression of five iron regulation-related genes, *BMPER*, *BMP6*, *FTH1*, *HAMP*, and *SLC40A1* in SUGP2 knockdown cells (Figure S5A, Table S9). Specifically, as *CIRBP* V1/V3 did not regulate *FTH1* and *SLC40A1*, whereas *BMP6* is mainly expressed in liver sinusoidal endothelial cells (LSECs) and is a binding protein of BMPER (Figure S5B-D), we focused on BMPER and qRT-PCR confirmed the significant increase of *BMPER* expression in SUGP2 knockdown Huh-7 (Figure 2A), and notably, the *CIRBP* knockdown suppressed the expression of BMPER and improved pSMAD1/5 and *HAMP* levels in SUGP2-sienced Huh-7 cells (Figure 2B-D, Figure S6A). Specifically, in the *CIRBP* V1-transfected but not V3-transfected cells, we found that the *BMPER* expression was increased in both mRNA and protein levels, meanwhile, pSMAD1/5 protein levels and the *HAMP* expression were

decreased (Figure 2E-G, Figure S6B). Notably, mRNA stability assay showed that *CIRBP* V1 increased the level of *BMPER* mRNA in Huh-7 cells after treatment with actinomycin D for 24 h

(Figure 2H). Therefore, *CIRBP* V1 may increase the mRNA stability and translation of *BMPER* and thereby inhibits BMP-SMAD signaling and *HAMP* expression.

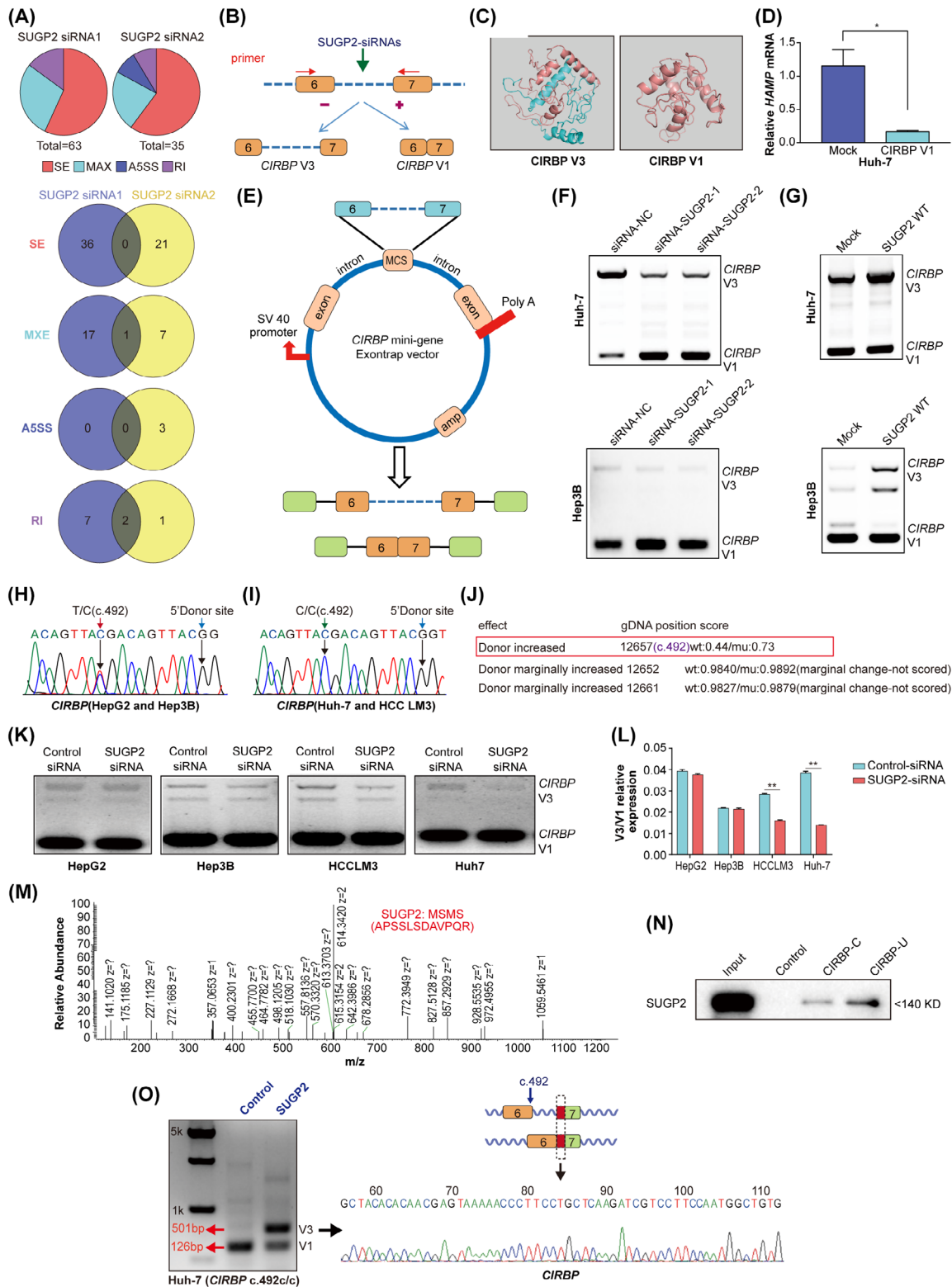


FIGURE 1 Legend on next page.

3.4 | The SUGP2 p.(Arg639Gln) variant increases the level of CIRBP V1, leading to up-regulated BMPER mRNA and protein expression, and the inhibition of pSMAD1/5 and HAMP levels

To further investigate the mechanism by which the SUGP2 p.(Arg639Gln) variant is involved in iron metabolism, we analyzed CIRBP V1 and BMPER expression in SUGP2 p.(Arg639Gln) plasmid transfected Huh-7 cells. Minigene assays showed the SUGP2 p.(Arg639Gln) variant increased the level of CIRBP V1 (Figure 2I, Figure S7A,B), which was consistent with what was observed in SUGP2 siRNA treated cells. Moreover, increased expression in both BMPER mRNA and BMPER protein levels was observed in SUGP2 p.(Arg639Gln) mutant cells (Figure 2J,L, Figure S7C), as the upregulated BMPER mRNA in SUGP2-silenced cells (Figure 2A). Similar to observed in CIRBP1 treated cells, no significant change of FTH1 and SLC40A1 expression but increased BMP6 expression were observed in SUGP2 p.(Arg639Gln) plasmid transfected Huh-7 cells (Figure S8A–C). We also found that pSMAD1/5 protein and HAMP mRNA levels were significantly decreased in SUGP2 p.(Arg639Gln) cells (Figure 2K,L, Figure S7C). Notably, significantly higher BMPER and lower pSMAD1/5 and HAMP expression were observed in cells with SUGP2 p.(Arg639Gln) variant but not in BMPER knockdown cells (Figure 2M–O, Figure S9). However, increased HAMP and pSMAD1/5 expression was not observed by the dual function of SUGP2 overexpression and BMPER knockdown (Figure 2N,O). In addition, mRNA stability assay also showed the SUGP2 p.(Arg639Gln) increased the level of BMPER mRNA in Huh-7 cells after treatment with actinomycin D for 24 h (Figure 2P). Therefore, the SUGP2 p.(Arg639Gln) variant may increase the mRNA stability and translation of BMPER and thereby inhibit BMP-SMAD signaling and HAMP expression.

3.5 | SUGP2^{R622Q} mice showed down-regulated HAMP expression and more iron overload in mice fed an iron-rich diet

To further verify the role of the SUGP2 p.(Arg639Gln) variant in iron overload, an SUGP2^{R622Q} mouse model was generated

(Figure S10). We next investigated the iron-regulation function of SUGP2 p.(Arg622Gln) variant and performed a detailed analysis of the iron metabolism phenotype (Figure 3A). Prussian blue staining of mice liver tissue showed significant differences in liver iron overload between SUGP2^{WT} and SUGP2^{R622Q} mice fed 2% iron diet for 3 days and 2 weeks (Figure 3B), which is consistent with the results of iron ion detection in liver tissues of 2 weeks high-iron mice (Figure 3C), and the serum ferritin and iron were also elevated in SUGP2^{R622Q} mice (Figure 3D,E). Reduced hepcidin levels were observed in the serum of SUGP2^{R622Q} mice fed 2% iron diet for 2 weeks (Figure 3F). In addition, we found that *Bmp6* and *Hamp* mRNA levels were significantly decreased in the liver of SUGP2^{R622Q} mice fed 2% iron diet for 2 weeks (Figure 3G,H). However, compared with SUGP2^{WT} mice, the SUGP2^{R622Q} mice displayed no significant difference in serum ALT/AST levels, and obvious liver injury or fibrosis in SUGP2^{R622Q} mice fed 2% iron diet for 2 weeks (Figure S11). Anyway, our animal study indicated that the mutant SUGP2 may function in the suppression of *Hamp* expression and the induction of iron overload.

We also generated SUGP2 knockout (SUGP2^{-/-}) mice (Figure S12), which also showed the down-regulated *Hamp* expression and more iron overload in mice fed an iron-rich diet (Figure S13A–E).

3.6 | The SUGP2 p.(Arg622Gln) variant in mice may down-regulate the Bmp/Smad pathway via Cirbp/Bmper

To further validate the functional effect of the SUGP2 p.(Arg622Gln) variant in vivo, we analyzed Bmper expression and the Bmp/Smad pathway in the SUGP2^{R622Q} mice. Compared with SUGP2^{WT} mice, more up-regulated Bmper and Fth1 expression and down-regulated p-Smad1/5 and *Bmp6* expression were observed in SUGP2^{R622Q} mice fed 2% iron diet for 2 weeks but not in the mice fed 2% iron diet for 3 days or with normal diet, and the similar results were observed in the SUGP2^{-/-} mice (Figure 3I,J, Figure S13F–H). RT-PCR and IHC analysis revealed higher

FIGURE 1 SUGP2 knockdown caused abnormal alternative splicing of CIRBP pre-mRNA, resulting in an increased normal splicing form of CIRBP V1 associated with down-regulation of HAMP expression, and CIRBP c.492 C/C genotype was more susceptible for SUGP2 function. (A) Depiction of four RNA splicing events in cells transfected with two SUGP2 siRNAs. Venn diagram showing the common RNA splicing-related genes in cells transfected with the two SUGP2 siRNAs. (B) Schematic diagram represents CIRBP pre-mRNA splicing. (C) Spatial structure of CIRBP V1 and V3 protein; (D) Quantitative RT-PCR analysis of HAMP expression in CIRBP V1 plasmid transfected cells. GAPDH was used as the internal control. (E) Schematic diagram showing construction of the CIRBP mini-gene exon-trap vectors. (F) and (G) Agarose gel electrophoresis of CIRBP transcripts of the mini-gene assays showing CIRBP transcript V1 and V3 content in SUGP2 knockdown and SUGP2 over-expressed Huh-7 and Hep3B cells. (H) and (I) Sanger sequencing of CIRBP exon 6–7 in HepG2 and Hep3B (H) and Huh-7 and HCCLM3 cells (I), differences in base sequences are indicated by arrows (c.492). (J) MatationTaster software predicts CIRBP c.492 site is a potential splicing site for CIRBP pre-mRNA. (K) and (L) Agarose gel electrophoresis of the CIRBP RT-PCR products from HepG2, Hep3B, HCCLM3, and Huh-7 cells (K). Quantitative ratio analysis of CIRBP transcripts V1 and V3 in different cells (L). (M) Mass spectrometry (MS) assays of protein binding to the CIRBP RNA oligomers identified a SUGP2 protein fragment. (N) The SUGP2 protein binding to CIRBP mutant (c.492) or wild-type RNA oligomers (CIRBP-C and CIRBP-U) probes was detected by Western blot with a SUGP2 antibody. (O) RNA immunoprecipitation assays were used to analyze the interaction of SUGP2 protein and CIRBP transcripts. Agarose gel electrophoresis of CIRBP RT-PCR products and Sanger sequencing showed increased CIRBP V3 in SUGP2 over-expressed cell and the identification of the CIRBP transcripts common sequence. A5SS, alternative 5' splice site; MXE, mutually exclusive exons; RI, retained intron; SE, skipped exon. [Color figure can be viewed at wileyonlinelibrary.com]

expression of both *Bmper* mRNA and protein in the liver of *Sugp2*^{R622Q} mice than in *Sugp2*^{WT} mice (Figure 3K,L). Notably, although the *Cirbp* gene sequence around c.492 is different between mouse and human, a higher *Cirbp* V1/V3 transcript ratio was observed in the liver of *SUGP2*^{R622Q} mice than in *Sugp2*^{WT} mice (Figure 3M,N).

3.7 | High rate of the *SUGP2* p.(Arg639Gln) variant identified in primary iron overload cases with *CIRBP* c.492 C/C and increased expression of BMPER

Sanger sequencing identified variant c.1916 G>A [p.(Arg639Gln)] in exon 5 of *SUGP2* in 10 of 54 (18.5%) primary iron overload cases

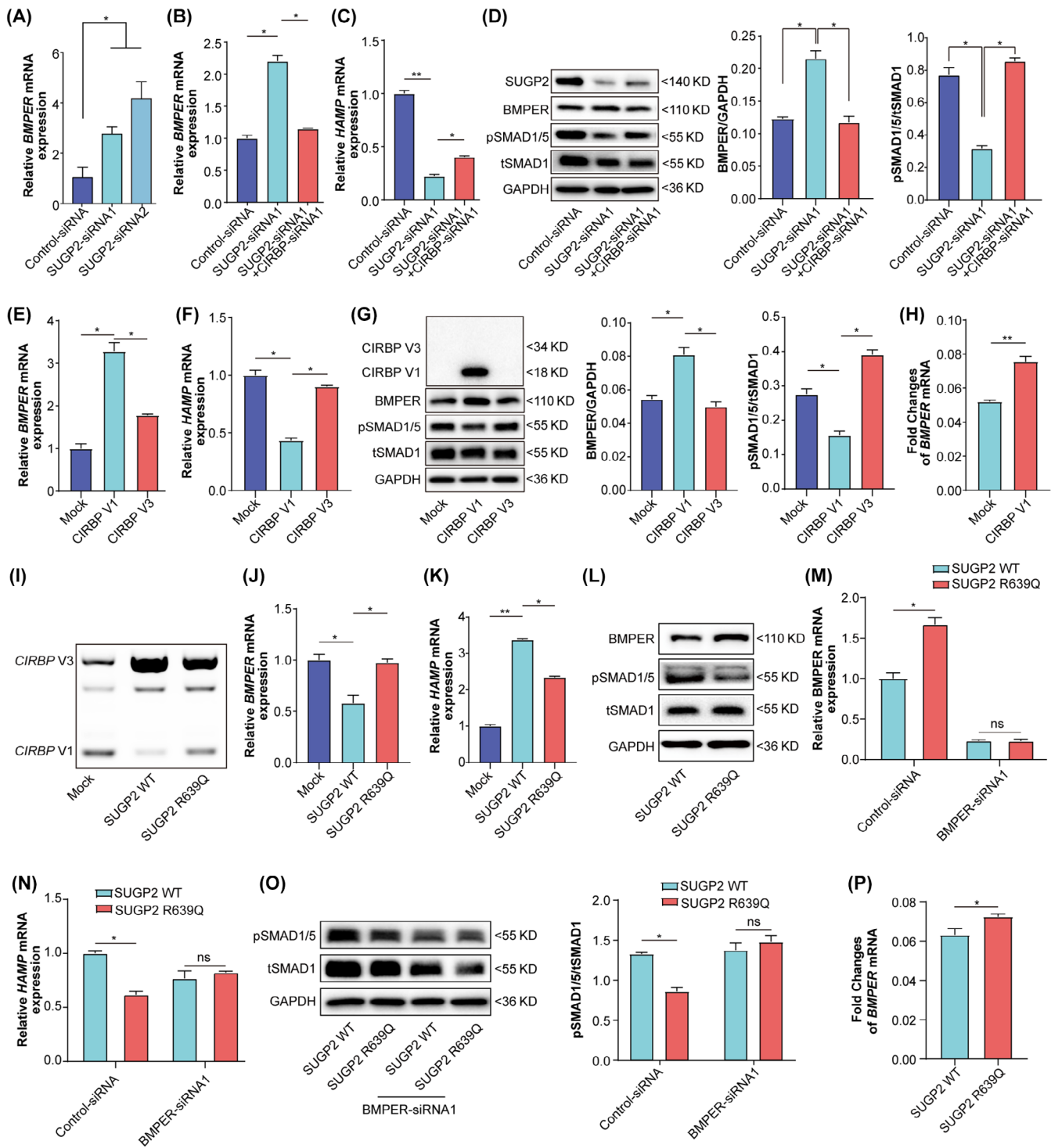


FIGURE 2 Legend on next page.

(Figure 4A,B, Table S10). Sequence comparison showed that residue 639 of *SUGP2* is conserved among different species (Figure 4C).

One patient was homozygous for *SUGP2* p.(Arg639Gln), while other patients carried only a single *SUGP2* p.(Arg639Gln) heterozygous variant. Exome sequencing of five cases with a single *SUGP2* p.(Arg639Gln) heterozygous variant (S4, S5, S6, S8, S9) identified heterozygous variants in the other iron metabolism-related genes in all five patients (Table S11).

Abdominal magnetic resonance imaging (MRI) revealed iron overload in the liver with different degree; representative results of patient S2 homozygous for the p.(Arg639Gln) variant and patient S3 heterozygous for the *SUGP2* p.(Arg639Gln) variant were shown in Figure 4D. Iron staining in patient S2 showed severe iron deposition in the liver, whereas patient S3 had mild hepatic iron (Figure 4E). Immunohistochemical staining of BMPER revealed significant up-regulation in patient S2 and S3 (Figure 4F).

As the target gene of *SUGP2*, the sequence between *CIRBP* exon 6 and 7 was sequenced in the cases with primary iron overload. All cases carrying *SUGP2* p.(Arg639Gln) had the *CIRBP* c.492 C/C genotype (Figure 4G).

4 | DISCUSSION

Hemochromatosis morbidity in Asian countries is rarely reported, and the general pattern of variant in haemochromatosis-related genes in these populations remains to be explored. Through a multicenter study, we recently identified a series of variants in non-*HFE* genes in hemochromatosis,^{7,15,16} and by whole exome sequencing, we identified a high rate of p.(Arg639Gln) variant in the *SUGP2*, a known splicing-related factor that is associated with regulation of the BMP/SMAD pathway and *HAMP* levels.¹⁵ In the present study, we identified *CIRBP* to be a target gene for *SUGP2* splicing function as an inhibitor factor; the *SUGP2* p.(Arg639Gln) variant may lead to an increased normal splicing form of *CIRBP* V1. The *CIRBP* V1 increased the mRNA stability and translation of *BMPER*, and thereby down-regulated pSMAD1/5 and *HAMP*

expression. This may constitute a major etiological factor of hemochromatosis in China.

SUGP2 is a component of the spliceosome and may be involved in the abnormal splicing of the *ISCU* gene, a causative gene of hereditary myopathy with lactic acidosis, as one of the splicing-related factors.^{18,19} However, the exact role of *SUGP2* in pre-mRNA splicing, as well as the target gene of *SUGP2* and the subsequent effect on signaling associated with the regulation of iron metabolism remains unknown. To investigate the pathogenic role of *SUGP2* p.(Arg639Gln) variant in hemochromatosis, we performed RNA-seq-based AS analysis of *SUGP2* knockdown cells and identified *CIRBP* as the target gene for *SUGP2*. Furthermore, RNA-seq analysis identified several known iron metabolism-related genes among hundreds of significant up- or down-regulator genes, and subsequently analysis identified BMPER and its binding protein BMP6, which was mainly expressed in LSECs, but not FTH1 and SLC40A1 as the downstream gene of *CIRBP*. *CIRBP* is a RNA-binding protein that can promote the stability of mRNAs of downstream genes.^{26,27} Our results showed that increased levels of *CIRBP* V1 may increase the stability and translation of *BMPER* mRNA, a known competitive inhibitor of BMP-SMAD signaling, and negatively regulated pSMAD1/5 and hepcidin expression.^{28,29} Therefore, BMPER is probably the main factor involved in the regulation of iron metabolism by *SUGP2*, and *SUGP2* may regulate iron metabolism through the *SUGP2*/*CIRBP*/*BMPER* axis.

In the present study, *CIRBP* was identified as the target gene for *SUGP2* splicing. It is interesting that *CIRBP* is located at 19p13.3, very close to the *SUGP2* gene, which is located at 19p13.11, indicating the possibility of clustering of functionally related genes.³⁰ *CIRBP* is induced after cells are exposed to a moderate cold shock and is responsible for the post-transcriptional regulation of specific genes, while other cell stresses, such as ultraviolet light radiation and hypoxia, can also increase its expression.²⁷ Under stress conditions, *CIRBP* can regulate its own expression by self-transcriptional activation of alternative promoters.²⁷ After relocating to the cytoplasm from the nucleus, *CIRBP* assists cells in adapting to novel environmental conditions by stabilizing specific mRNAs and facilitating their translation through interaction with the 5'- or 3'-UTRs of target

FIGURE 2 *SUGP2* knockdown and the *SUGP2* p.(Arg639Gln) variant increased BMPER, *CIRBP* V1, and *HAMP* expression, and the *CIRBP* V1 increased the mRNA stability and translation of *BMPER* and inhibited BMP-SMAD signaling. (A) Quantitative RT-PCR analysis of *BMPER* in *SUGP2* silenced cells. GAPDH was used as the internal control. (B) and (C) Quantitative RT-PCR analysis of *BMPER* and *HAMP* mRNA in *SUGP2*-siRNA cells with *CIRBP*-siRNA treatment. (D) Western blot and densitometric analysis of BMPER and pSMAD1/5 proteins in *SUGP2*-siRNA cells with *CIRBP*-siRNA treatment. (E) and (F) Quantitative RT-PCR analysis of *BMPER* and *HAMP* mRNA in *CIRBP*-V1- and *CIRBP*-V3-transfected cells. (G) Western blot and densitometric analysis of *CIRBP*, BMPER, pSMAD1/5, and tSMAD1 proteins in extracts from *CIRBP*-V1 and *CIRBP*-V3-transfected and control cells. (H) Analysis of mRNA stability of *BMPER*. *BMPER* mRNA levels in the *CIRBP* V1 transfected cells treated with actinomycin D were detected by q-RT-PCR. Fold changes were calculated as the ratio of *BMPER* mRNA levels at 24 and 0 h. (I) Agarose gel electrophoresis of the RT-PCR products obtained from *CIRBP* mRNA showed the expression of *CIRBP* transcript V1 and V3 in *SUGP2* p.(Arg639Gln) cells compared with that in *SUGP2* WT cells. (J) and (K) mRNA levels of *BMPER* and *HAMP* in cells transfected with *SUGP2* and *SUGP2* p.(Arg639Gln) plasmids detected by quantitative RT-PCR. (L) Protein levels of BMPER and pSMAD1/5 were analyzed by western blot. GAPDH was used as the loading control. (M) and (N) mRNA levels of BMPER and *HAMP* in BMPER-siRNA cells transfected with *SUGP2* and *SUGP2* p.(Arg639Gln) plasmid detected by quantitative RT-PCR. (O) Protein levels of pSMAD1/5 in BMPER-siRNA cells transfected with *SUGP2* and *SUGP2* p.(Arg639Gln) plasmid detected by Western blot. (P) Analysis of mRNA stability of *BMPER*. *BMPER* mRNA levels in the *SUGP2* and *SUGP2* p.(Arg639Gln) plasmid transfected cells treated with actinomycin D were detected by q-RT-PCR. Fold changes were calculated as the ratio of *BMPER* mRNA levels at 24 and 0 h. (**P* < .05; ***P* < .01). [Color figure can be viewed at wileyonlinelibrary.com]

gene mRNAs.^{26,27,31} CIRBP has been reported involved in multiple processes, such as the stress response, carcinogenesis, the inflammatory response, cell cycle progression, and cell adhesion.^{21,22,32,33} However, no study has reported its role in an inherited metabolic disorder. The present reported for the first time that the CIRBP was involved in

the regulation of iron metabolism, and consistently, the CIRBP V1 may increase the expression and translation of *BMPER* through the stabilization of *BMPER* mRNA.

To further explore the underlying mechanism of *SUGP2* on *CIRBP* pre-mRNA AS and if there is a potential site related to the splicing of

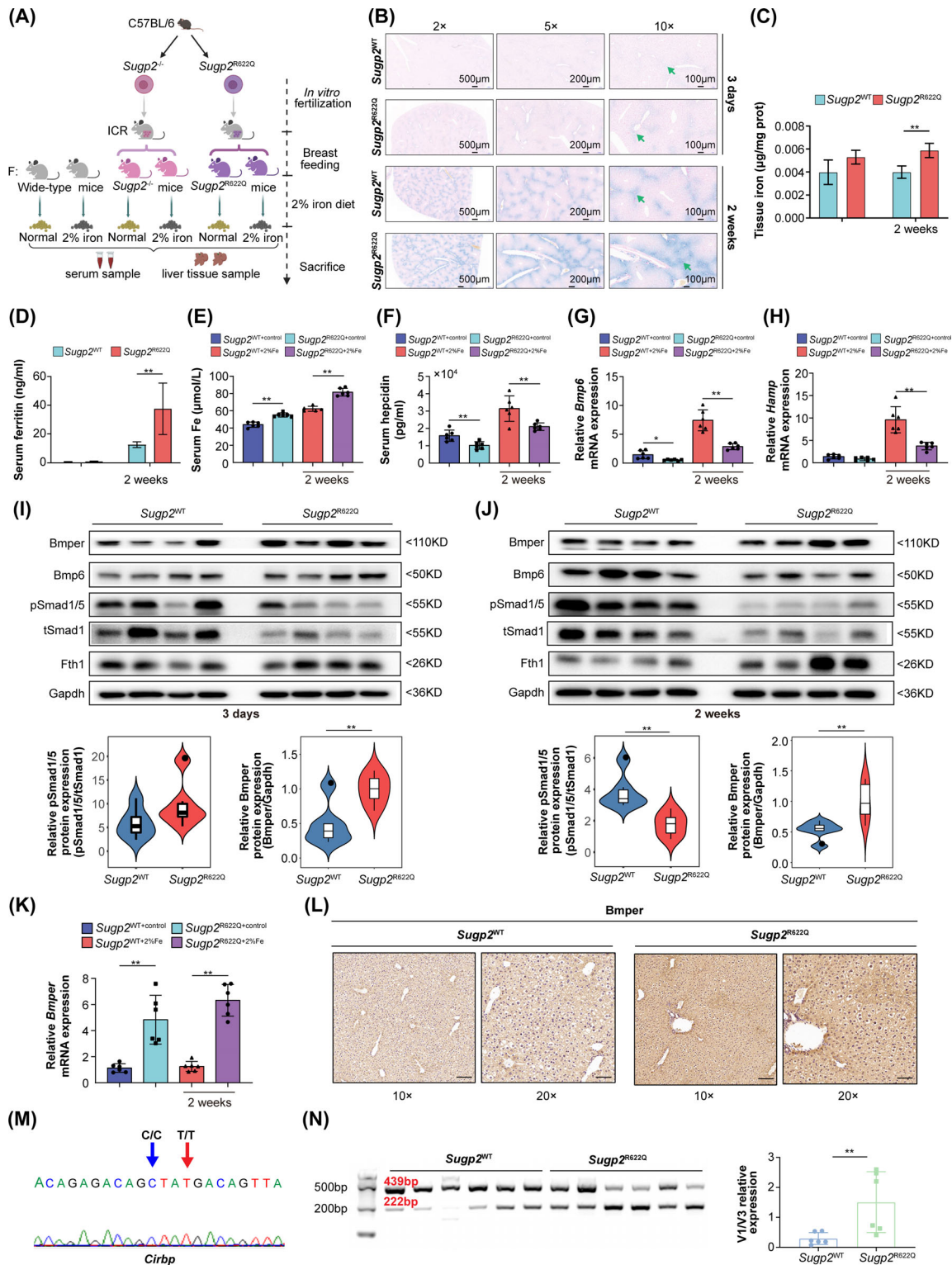


FIGURE 3 Legend on next page.

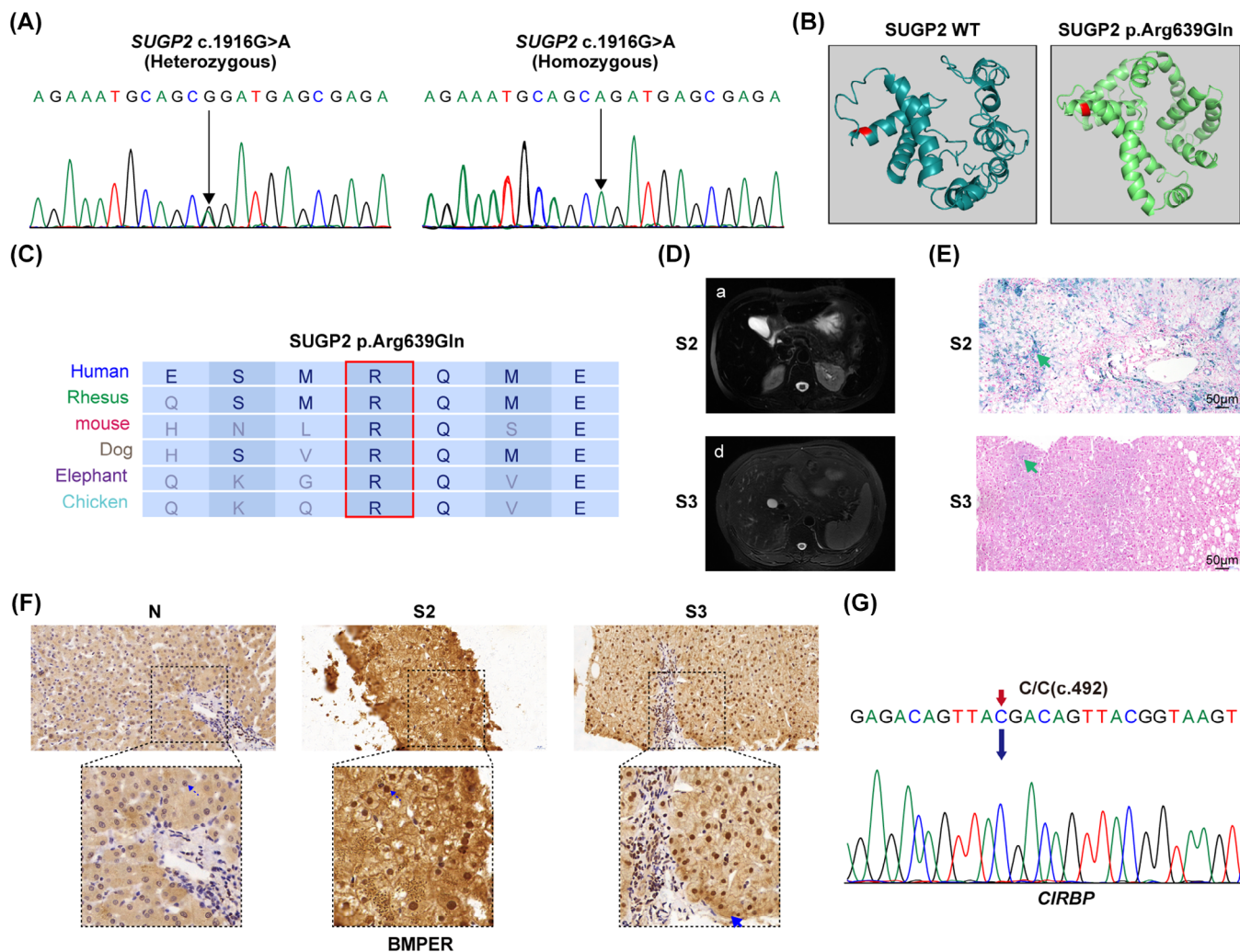


FIGURE 4 High rate of the *SUGP2* p.(Arg639Gln) variant in hemochromatosis cases with *CIRBP* c.492 C/C and increased expression of BMPER. (A) Representative sequencing of the missense variant c.1916G>A, p.(Arg639Gln) in exon 5 of *SUGP2* in patients with primary iron overloads. (B) Spatial structure of p.(Arg639Gln) *SUGP2* protein; (C) Alignment of residue sequences of human, rhesus, mouse, dog, elephant, and chicken *SUGP2* with regions flanking the p.(Arg639Gln) variant site. The position of the p.(Arg639Gln) variant was indicated by the red box. Alignment was performed by <http://genome.ucsc.edu/>. (D) MRI of patient S2 with homozygous *SUGP2* p.(Arg639Gln) showed low signal intensity in the liver and spleen in a T2-weighted image showing severe iron overload in the liver and spleen, whereas the MRI of patient S3 with heterozygous *SUGP2* p.(Arg639Gln) showed low signal intensity in the liver but normal signal intensity in the spleen in a T2-weighted image indicating iron overload in the liver but not in the spleen. (E) Liver Fe staining (Prussian blue) of patients S2 and S3. (F) BMPER immunohistochemistry in the liver tissue of patients S2 and S3. (G) Representative sequencing between *CIRBP* exon 6 and 7 in the cases with primary iron overload. [Color figure can be viewed at wileyonlinelibrary.com]

FIGURE 3 *Sugp2*^{R622Q} variant knock-in mice suppress *Hamp* expression and induced more iron overload in mice fed an iron-rich diet, and the *SUGP2* p.(Arg622Gln) variant in mice may down-regulate the Bmp/Smad pathway via *Cirbp*/Bmper. (A) The schematic diagram of the animal experiment. (B) Prussian blue staining in 4 μ m paraffin sections of livers from *Sugp2*^{WT} and *Sugp2*^{R622Q} mice fed iron for 3 days and 2 weeks, respectively. Scale bars: 500 μ m; 200 μ m; 100 μ m. Blue represents iron staining (green arrow). (C) Enzymatic-based iron content measurement in liver extracts from *Sugp2*^{WT} and *Sugp2*^{R622Q} mice fed iron for 3 days and 2 weeks. (D) Enzyme-linked immunosorbent assay (ELISA) for determination of serum ferritin concentration in mice. (E) and (F) Serum iron and hepcidin concentration in *Sugp2*^{WT} and *Sugp2*^{R622Q} mice fed with or without 2% iron diet for 2 weeks. (G) and (H) Real-time RT-PCR analysis of liver *Bmp6* and *Hamp* mRNAs from *Sugp2*^{WT} and *Sugp2*^{R622Q} mice fed iron for 2 weeks. (I) and (J) Representative Western blot assays for the detection of Bmper, Bmp6, pSmad1/5, tSmad1, and Fth1 proteins expression in the liver of *Sugp2*^{R622Q} mice fed iron for 3 days and 2 weeks. (K) Hepatic *Bmper* mRNA levels were measured in the indicated mice. (L) Measurement of liver Bmper levels by immunohistochemistry. The scale bars are 100 and 50 μ m. (M) Sanger sequencing of *Cirbp* exon 6–7. (N) Agarose gel electrophoresis of *Cirbp* V1 and V3 transcripts in *Sugp2*^{WT} and *Sugp2*^{R622Q} mice. *Cirbp* transcript V1/V3 quantification ratio was shown. (**P* < .05; ***P* < .01). [Color figure can be viewed at wileyonlinelibrary.com]

CIRBP pre-mRNA, we conducted sequencing of *CIRBP* between exon 6 and 7 in a series of cell lines. Our in vitro study confirmed that *SUGP2* leads to abnormal splicing of *CIRBP* pre-mRNA by the splice site variant at *CIRBP* c.492, and the *CIRBP* c.492 C/C genotype is more susceptible to *SUGP2* function. Notably, although the sequences around *CIRBP* c.492 were different among different species, such as human, mouse, rat, and zebrafish, our *Sugp2*^{R622Q} mice model showed that the *SUGP2* p.(Arg622Gln) variant resulted in increased *Cirbp* V1 transcripts and the negative regulation of corresponding downstream hemochromatosis-related pathways. However, further study in animal models will help determine the detailed mechanism of the *CIRBP* c.492 in abnormal *Cirbp* splicing.

Our RNA-seq analysis also identified *BMPER* as a downstream gene of *SUGP2*. *BMPER* can suppress hepcidin promoter activity and reduce hepcidin levels in liver cells as a competitive inhibitor of the BMP/SMAD pathway.^{29,34} *Bmper* binds to *Bmp6* inhibiting BMP signaling, and soluble *Bmper* is a negative regulator of *HAMP* and inhibiting BMP signaling and thus down-regulate *Hamp* expression in mice.³⁴ Notably, as in some situations, *Bmper* has been shown to elicit pro-BMP responses, a function that may be dependent on whether the protein is membrane-associated or soluble. In this respect, *BMPER* may function in the manner that the soluble form is anti-BMPs and membrane form is pro-BMP.^{34,35} Thus, in *Sugp2* R622Q and *Sugp2* Knockout mice, the soluble *Bmper* expression may inhibit BMP signaling and down-regulate *Hamp* whereas the membrane form of *BMPER* may promote *BMP6* expression, as observed in the *SUGP2* knockdown Huh-7 cell.

In addition, the level of *BMP6* in vivo exhibits mis-regulation when the BMP signaling pathway has been disrupted. For example, in *HJV* knockout mouse, hepatic *BMP6* expression increases significantly, and hepatic *BMP6* mRNA expression is closely correlated with hepatic iron loading but the regulation of hepatic *BMP6* expression by iron is independent of *HJV*.³⁶ As a BMP antagonist, *BMPER* may also affect the expression of *BMP6* in vivo probably due to BMP signaling pathway was hampered. However, the expression of *BMP6* was significantly increased after *SUGP2* knockdown in vitro. Therefore, there may be another possibility that the down-regulation of *BMP6* in *SUGP2* mutant mice may not directly due to the *SUGP2*, and the detail mechanism needs to be further explored. Anyway, the anti-BMPs characteristics of *BMPER* may constitute the main cause of hepcidin deficiency and iron overload in *SUGP2* knockout and mutant mice. Our in vitro and in vivo models confirmed that the *SUGP2* p.(Arg639Gln) variant may up-regulate the expression of *BMPER* via *CIRBP* and was consistent with what was observed in hemochromatosis patients with *SUGP2* p.(Arg639Gln) variant and increased *BMPER* expression.

As the major pathogenic factor for hemochromatosis, the *HFE* p.C282Y variant was identified in approximately 5% of the general Caucasian population³⁷ but rarely reported in the East-Asian population (0.0001 in gnomAD database). Similarly, the *SUGP2* p.(Arg639Gln) heterozygous variant was identified in 5% of the general Chinese population (5/100, data not shown) but is rare in the general Caucasian population (0.0003 in a non-Finnish European population in gnomAD database). Notably, most patients were only heterozygous for *SUGP2* p.(Arg639Gln). However, exome sequencing identified heterozygous

variants in other iron metabolism-related genes that directly or indirectly correlate with iron metabolism,^{7,17,38,39} indicating a variant pattern combining heterozygosity for *SUGP2* p.(Arg639Gln) with variants in other iron metabolism-related genes, as observed in the pedigree analysis of patients H1, H25, H35 in our previous study.¹⁵

Notably, the present study identified *CIRBP* c.492 C/C genotypes in all hemochromatosis cases that carried *SUGP2* p.(Arg639Gln). Interestingly, the NCBI genomeAD database shows the allele frequency of *CIRBP* c.492 C to be 0.9807 in an Eastern-Asian population but 0.7732 in a non-Finnish European population, indicating that although *CIRBP* c.492 C/C may not lead to the hemochromatosis disease phenotype, *SUGP2* p.(Arg639Gln) may result in alternative *CIRBP* transcripts and may therefore increase the risk for hemochromatosis, especially in Asian populations.

In summary, *SUGP2* functioned as a splicing inhibitor factor and may regulate iron metabolism through the *SUGP2*/*CIRBP*/*BMPER* axis, and the *SUGP2* p.(Arg639Gln) variant may be one of the major etiological factors of hemochromatosis in China.

AUTHOR CONTRIBUTIONS

Jian Huang, Jidong Jia, and Changfa Fan conceptualized and/or supervised the study. Yanmeng Li, Anjian Xu, and Susu Liu performed the most experiments. Anjian Xu and Donghu Zhou provided technique support. Wei Zhang, Wei Geng, Yiming Zhou, Xinyan Zhao, and Xiaojuan Ou provided patients' samples and clinical data and analyzed and interpreted the data. Yanmeng Li, Anjian Xu, Qin OuYang, Huaduan Zi, and Bei Zhang did the experiments and analyzed and interpreted the data. Xinyan Zhao, Xiaoming Wang, Weijia Duan, and Ning Zhang provided, analyzed, and interpreted patients' samples and clinical data. Yanmeng Li, Anjian Xu, and Susu Liu wrote the manuscript. Jian Huang, Jidong Jia, and Changfa Fan revised the manuscript. All authors have read and approved the final manuscript.

FUNDING INFORMATION

This study was supported by the National Natural Science Foundation of China (no. 81974072), grants from the Beijing Municipal Natural Science Foundation (nos. 7132058 and 7202034), and Digestive Medical Coordinated Development Center of Beijing Municipal Administration of Hospitals (XXX0101 and XXZ0502).

CONFLICT OF INTEREST STATEMENT

The authors disclose no conflicts of interest.

DATA AVAILABILITY STATEMENT

The data that support the findings of this study are available from the corresponding author upon reasonable request.

PATIENT CONSENT STATEMENT

Patients provided consent through an Institutional Review Board-approved protocol to provide blood and liver biopsy samples, which were obtained by approval of an investigator protocol by the Clinical Research Ethics Committee of Beijing Friendship Hospital, Capital Medical University.

ORCID

Yanmeng Li  <https://orcid.org/0000-0003-3151-7099>

Anjian Xu  <https://orcid.org/0000-0003-4186-9485>

Jian Huang  <https://orcid.org/0000-0002-5180-9833>

REFERENCES

- Adams PC, Jeffrey G, Ryan J. Haemochromatosis. *Lancet*. 2023;401(10390):1811-1821.
- Powell LW, Seckington RC, Deugnier Y. Haemochromatosis. *Lancet*. 2016;388(10045):706-716.
- Wang CY, Babitt JL. Liver iron sensing and body iron homeostasis. *Blood*. 2019;133(1):18-29.
- Chen J, Li X, Ge C, Min J, Wang F. The multifaceted role of ferroptosis in liver disease. *Cell Death Differ*. 2022;29(3):467-480.
- Camaschella C, Nai A, Silvestri L. Iron metabolism and iron disorders revisited in the hepcidin era. *Haematologica*. 2020;105(2):260-272.
- Turshudzhyan A, Wu DC, Wu GY. Primary non-HFE hemochromatosis: a review. *J Clin Transl Hepatol*. 2023;11(4):925-931.
- Zhang W, Li Y, Xu A, et al. Identification of novel non-HFE mutations in Chinese patients with hereditary hemochromatosis. *Orphanet J Rare Dis*. 2022;17(1):216.
- Hsu CC, Senussi NH, Fertrin KY, Kowdley KV. Iron overload disorders. *Hepatol Commun*. 2022;6(8):1842-1854.
- Kong X, Xie L, Zhu H, et al. Genotypic and phenotypic spectra of hemojuvelin mutations in primary hemochromatosis patients: a systematic review. *Orphanet J Rare Dis*. 2019;14(1):171.
- McDonald CJ, Wallace DF, Crawford DH, Subramaniam VN. Iron storage disease in Asia-Pacific populations: the importance of non-HFE mutations. *J Gastroenterol Hepatol*. 2013;28(7):1087-1094.
- Chen SR, Yang LQ, Chong YT, et al. Novel gain of function mutation in the SLC40A1 gene associated with hereditary haemochromatosis type 4. *Intern Med J*. 2015;45(6):672-676.
- Wang Y, Du Y, Liu G, et al. Identification of novel mutations in HFE, HFE2, TFR2, and SLC40A1 genes in Chinese patients affected by hereditary hemochromatosis. *Int J Hematol*. 2017;105(4):521-525.
- Huang FW, Rubio-Aliaga I, Kushner JP, Andrews NC, Fleming MD. Identification of a novel mutation (C321X) in HJV. *Blood*. 2004;104(7):2176-2177.
- Tang S, Bai L, Gao Y, et al. A novel mutation of transferrin receptor 2 in a Chinese pedigree with type 3 hemochromatosis: a case report. *Front Genet*. 2022;13:836431.
- Lv T, Zhang W, Xu A, et al. Non-HFE mutations in haemochromatosis in China: combination of heterozygous mutations involving HJV signal peptide variants. *J Med Genet*. 2018;55(10):650-660.
- Zhang W, Xu A, Li Y, et al. A novel SLC40A1 p.Y333H mutation with gain of function of ferroportin: a recurrent cause of haemochromatosis in China. *Liver Int*. 2019;39(6):1120-1127.
- Li Y, Xu A, Ouyang Q, et al. DENND3 p.L708V activating variant is involved in the pathogenesis of hereditary hemochromatosis via the RAB12/TFR2 signaling pathway. *Hepatol Int*. 2023;17(3):648-661.
- Sampson ND, Hewitt JE. SF4 and SFRS14, two related putative splicing factors on human chromosome 19p13.11. *Gene*. 2003;305(1):91-100.
- Nordin A, Larsson E, Holmberg M. The defective splicing caused by the ISCU intron mutation in patients with myopathy with lactic acidosis is repressed by PTBP1 but can be derepressed by IGF2BP1. *Hum Mutat*. 2012;33(3):467-470.
- Kim MJ, Yu CY, Theusch E, et al. SUGP1 is a novel regulator of cholesterol metabolism. *Hum Mol Genet*. 2016;25(14):3106-3116.
- Corre M, Lebreton A. Regulation of cold-inducible RNA-binding protein (CIRBP) in response to cellular stresses. *Biochimie*. 2024;217:3-9.
- Xiao X, Zhang W, Hua D, et al. Cold-inducible RNA-binding protein (CIRBP) promotes porcine reproductive and respiratory syndrome virus (PRRSV)-induced inflammatory response. *Int Immunopharmacol*. 2020;86:106728.
- Indacochea A, Guerrero S, Urena M, et al. Cold-inducible RNA binding protein promotes breast cancer cell malignancy by regulating Cystatin C levels. *RNA*. 2021;27(2):190-201.
- Bacon BR, Adams PC, Kowdley KV, Powell LW, Tavill AS. American Association for the Study of liver D. Diagnosis and management of hemochromatosis: 2011 practice guideline by the American Association for the Study of Liver Diseases. *Hepatology*. 2011;54(1):328-343.
- Li Y, Ouyang Q, Chen Z, et al. Intracellular labile iron is a key regulator of hepcidin expression and iron metabolism. *Hepatol Int*. 2023;17(3):636-647.
- Liao Y, Tong L, Tang L, Wu S. The role of cold-inducible RNA binding protein in cell stress response. *Int J Cancer*. 2017;141(11):2164-2173.
- Siomi H, Dreyfuss G. RNA-binding proteins as regulators of gene expression. *Curr Opin Genet Dev*. 1997;7(3):345-353.
- Hasebe T, Tanaka H, Sawada K, et al. Bone morphogenetic protein-binding endothelial regulator of liver sinusoidal endothelial cells induces iron overload in a fatty liver mouse model. *J Gastroenterol*. 2017;52(3):341-351.
- Yan Y, Wang Q. BMP signaling: lighting up the way for embryonic dorsoventral patterning. *Front Cell Dev Biol*. 2021;9:799772.
- Xu H, Liu JJ, Liu Z, Li Y, Jin YS, Zhang J. Synchronization of stochastic expressions drives the clustering of functionally related genes. *Sci Adv*. 2019;5(10):eaax6525.
- Sakurai T, Itoh K, Higashitsuji H, et al. Cirp protects against tumor necrosis factor-alpha-induced apoptosis via activation of extracellular signal-regulated kinase. *Biochim Biophys Acta*. 2006;1763(3):290-295.
- Kim YM, Hong S. Controversial roles of cold-inducible RNA-binding protein in human cancer (review). *Int J Oncol*. 2021;59(5):91.
- Gao H, Xie R, Huang R, et al. CIRBP regulates pancreatic cancer cell ferroptosis and growth by directly binding to p53. *J Immunol Res*. 2022;2022:2527210.
- Patel N, Masaratana P, Diaz-Castro J, et al. BMPER protein is a negative regulator of hepcidin and is up-regulated in hypotransferrinemic mice. *J Biol Chem*. 2012;287(6):4099-4106.
- Zhang JL, Huang Y, Qiu LY, Nickel J, Sebald W. von Willebrand factor type C domain-containing proteins regulate bone morphogenetic protein signaling through different recognition mechanisms. *J Biol Chem*. 2007;282(27):20002-20014.
- Zhang AS, Gao J, Koeberl DD, Enns CA. The role of hepatocyte hemojuvelin in the regulation of bone morphogenic protein-6 and hepcidin expression in vivo. *J Biol Chem*. 2010;285(22):16416-16423.
- Brissoit P, Pietrangelo A, Adams PC, de Graaff B, McLaren CE, Loreal O. Haemochromatosis. *Nat Rev Dis Primers*. 2018;4:18016.
- Zhang X, Zhang J, Bauer A, et al. Fine-tuning BMP7 signalling in adipogenesis by UBE2O/E2-230K-mediated monoubiquitination of SMAD6. *EMBO J*. 2013;32(7):996-1007.
- Schwiebacher C, Serafin A, Zanon A, Pramstaller PP, Pichler I, Hicks AA. Involvement of proprotein convertase PCSK7 in the regulation of systemic iron homeostasis. *Hepatology*. 2013;58(5):1860-1861.

SUPPORTING INFORMATION

Additional supporting information can be found online in the Supporting Information section at the end of this article.

How to cite this article: Li Y, Xu A, Liu S, et al. SUGP2 p. (Arg639Gln) variant is involved in the pathogenesis of hemochromatosis via the CIRBP/BMPER signaling pathway. *Am J Hematol*. 2024;99(9):1691-1703. doi:10.1002/ajh.27377